



Contents lists available at ScienceDirect

NeuroImage

journal homepage: [www.elsevier.com/locate/neuroimage](http://www.elsevier.com/locate/neuroimage)

## Network analysis reveals disrupted functional brain circuitry in drug-naive social anxiety disorder

Xun Yang<sup>a,b,1</sup>, Jin Liu<sup>c,d,e,1</sup>, Yajing Meng<sup>f,1</sup>, Mingrui Xia<sup>c,d,e</sup>, Zaixu Cui<sup>c,d,e</sup>, Xi Wu<sup>a</sup>, Xinyu Hu<sup>a</sup>, Wei Zhang<sup>f</sup>, Gaolang Gong<sup>c,d,e</sup>, Qiyong Gong<sup>a,f,g,\*\*</sup>, John A. Sweeney<sup>a,h</sup>, Yong He<sup>c,d,e,\*</sup>

<sup>a</sup> Huaxi MR Research Center (HMRRRC), Department of Radiology, West China Hospital of Sichuan University, Chengdu, 610041, China

<sup>b</sup> Key Laboratory of Cognition and Personality of Ministry of Education, Faculty of Psychology, Southwest University, Chongqing, 400715, China

<sup>c</sup> National Key Laboratory of Cognitive Neuroscience and Learning, Beijing Normal University, Beijing, 100875, China

<sup>d</sup> Beijing Key Laboratory of Brain Imaging and Connectomics, Beijing Normal University, Beijing, 100875, China

<sup>e</sup> IDG/McGovern Institute for Brain Research, Beijing Normal University, Beijing, 100875, China

<sup>f</sup> Department of Psychiatry, West China Hospital of Sichuan University, Chengdu, 610041, China

<sup>g</sup> Department of Psychology, School of Public Administration, Sichuan University, Chengdu, 610065, China

<sup>h</sup> Department of Psychiatry and Behavioral Neuroscience, University of Cincinnati, Cincinnati, OH, 45219, USA

### ARTICLE INFO

#### Keywords:

Social anxiety disorder  
Connectome  
Graph theory  
Network-based statistics  
Frontolimbic

### ABSTRACT

Social anxiety disorder (SAD) is a common and disabling condition characterized by excessive fear and avoidance of public scrutiny. Psychoradiology studies have suggested that the emotional and behavior deficits in SAD are associated with abnormalities in regional brain function and functional connectivity. However, little is known about whether intrinsic functional brain networks in patients with SAD are topologically disrupted. Here, we collected resting-state fMRI data from 33 drug-naive patients with SAD and 32 healthy controls (HC), constructed functional networks with 34 predefined regions based on previous meta-analytic research with task-based fMRI in SAD, and performed network-based statistic and graph-theory analyses. The network-based statistic analysis revealed a single connected abnormal circuitry including the frontolimbic circuit (termed the “fear circuit”, including the dorsolateral prefrontal cortex, ventral medial prefrontal cortex and insula) and posterior cingulate/occipital areas supporting perceptual processing. In this single altered network, patients with SAD had higher functional connectivity than HC. At the global level, graph-theory analysis revealed that the patients exhibited a lower normalized characteristic path length than HC, which suggests a disorder-related shift of network topology toward randomized configurations. SAD-related deficits in nodal degree, efficiency and participation coefficient were detected in the parahippocampal gyrus, posterior cingulate cortex, dorsolateral prefrontal cortex, insula and the calcarine sulcus. Aspects of abnormal connectivity were associated with anxiety symptoms. These findings highlight the aberrant topological organization of functional brain network organization in SAD, which provides insights into the neural mechanisms underlying excessive fear and avoidance of social interactions in patients with debilitating social anxiety.

### Introduction

Social anxiety disorder (SAD) is one of the most common psychiatric conditions, with lifetime prevalence rates ranging between 7% and 13.3% (Stein and Stein, 2008). SAD typically emerges early in life, and

predicts psychiatric comorbidity, significant social function impairment, and persistent emotional, cognitive and behavioral disabilities (Ruscio et al., 2008). SAD is characterized by heightened anxiety, increased vigilance regarding negative social stimuli, and a bias toward perceiving social threat (Robinson et al., 2012). Emotional and cognitive

\* Corresponding author. National Key Laboratory of Cognitive Neuroscience and Learning, Beijing Key Laboratory of Brain Imaging and Connectomics, IDG/McGovern Institute for Brain Research, Beijing Normal University, China.

\*\* Corresponding author. Huaxi MR Research Center (HMRRRC), Department of Radiology, West China Hospital of Sichuan University, China.

E-mail addresses: [yong.he@bnu.edu.cn](mailto:yong.he@bnu.edu.cn) (Y. He), [qiyonggong@hmrrc.org.cn](mailto:qiyonggong@hmrrc.org.cn) (Q. Gong).

<sup>1</sup> These authors contributed equally to this work.

<https://doi.org/10.1016/j.neuroimage.2017.12.011>

Received 11 March 2017; Received in revised form 17 October 2017; Accepted 5 December 2017

Available online xxx

1053-8119/© 2017 Published by Elsevier Inc.

impairments associated with SAD have been linked to regional brain abnormalities and functional dysconnectivity among brain regions (Etkin and Wager, 2007; Mathew et al., 2001). Despite these advances in research, the functional integrity and topological organization of brain networks in patients with SAD remains largely unclear.

Task-based fMRI studies of SAD have most consistently indicated impairments in frontolimbic circuitry, in what has been termed the “fear circuit” (Etkin and Wager, 2007), which includes the dorsolateral prefrontal cortex (DLPFC), ventral medial prefrontal cortex (VMPFC), anterior cingulate cortex (ACC), amygdala, hippocampus, parahippocampus and the insula (Cremers et al., 2015; Gimenez et al., 2012; Guyer et al., 2008; Laeger et al., 2014; Prater et al., 2013; Robinson et al., 2014; Sladky et al., 2015; Stein et al., 2002). This neurocircuitry model has highlighted the roles of both emotional hyperactivity and reduced efficiency in the cognitive control of affect as key features of SAD. In addition, increased activity in medial parietal and occipital regions, which was evident in a recent meta-analysis (Bruhl et al., 2014), might underlie the enhanced environmental scanning for potentially threatening or feared stimuli in SAD. Whether a similar pattern of abnormality occurs in resting state brain physiology, which can be assessed by resting-state fMRI (R-fMRI), remains unknown.

One important unresolved issue is the relationship between impairments in the fear circuit and those in parietal and occipital perceptual systems, as they may be separate or integrated abnormalities. Furthermore, most identified aspects of altered connectivity were detected by traditional seed-based analysis rather than a network-based approach. The network-based statistic (NBS) analysis is recently developed tool for identifying network components that differ between groups (Zalesky et al., 2010), which can reveal both reduced (patients < HC) and increased (patients > HC) functional connectivity in brain networks.

The aim of this exploratory study was to use an unbiased data-driven framework for detecting abnormal functional connectivity and topological properties in brain regions linked previously to SAD. First, we focused on illness-relevant brain regions with previously established functional impairments in SAD based on meta-analytic studies of task-based fMRI research. We hypothesized that SAD patients would exhibit disrupted functional connectivity patterns and topological properties in these regions. To test this hypothesis, we recruited drug-naïve patients with SAD and evaluated their functional connectivity pattern disruption using a NBS analysis (Zalesky et al., 2010) and topological evaluation of intrinsic functional brain networks (global and regional properties) using a graph theory approach (Bullmore and Sporns, 2009; He and Evans, 2010; Rubinov and Sporns, 2010). We then examined relationships between disrupted topological organization and SAD symptom severity.

## Methods and materials

### Participants

Thirty-three drug-naïve patients with SAD were recruited from the outpatient department of West China Mental Health Centre, Chengdu, China. All of patients were determined by consensus of two experienced psychiatrists to currently meet diagnostic criteria for SAD following the administration of the Structured Clinical Interview for DSM Disorders (SCID using DSM-IV) (First MB et al., 1997). The patients had no previous psychopharmacological or psychological treatment, and no history of a psychotic disorder, bipolar disorder or major depression.

Thirty-three healthy controls (HC) were recruited from the local area via poster advertisements. The HC were pair-wise matched to the patients with SAD based on age and gender, and were screened using the SCID-Non-Patient Version to verify the absence of an Axis I disorder. This recruitment plan led to some healthy control subjects having notable levels of social anxiety but not meeting criteria for SAD. Exclusion criteria for all participants included a history of head injury, left handedness, neurological or systemic disease, or alcohol or drug abuse, or current pregnancy. Individuals were also excluded if they were less than 18 or

over 60 years to limit age-related effects in the data. Data from one healthy control was excluded due to large head movements during brain imaging (See “Data Preprocessing”). Ultimately, 33 drug-naïve patients with SAD and 32 HC were included in the study (Table 1).

Ratings of social anxiety during the past week were obtained using the self-administered Liebowitz Social Anxiety Scale (LSAS), a widely used clinical scale in SAD research (Baker et al., 2002; Fresco et al., 2001; Liebowitz et al., 1985). The LSAS provides assessment of both a fear factor (LSAS<sub>fear</sub>) and a social avoidance factor (LSAS<sub>avoidance</sub>). A total score (LSAS<sub>total</sub>) is derived by summing the LSAS<sub>fear</sub> and LSAS<sub>avoidance</sub> ratings. The study was approved by the local research ethics committee of Sichuan University, and written informed consent was obtained from all participants prior to study participation.

### MRI acquisition

MRI scans were performed on a 3.0 T MR scanner (Siemens Trio, Erlangen, Germany) with a 12-channel head coil as the signal receiver. Foam pads were used to restrict the head motion of the subjects. The R-fMRI data were obtained with the following gradient-echo planar imaging sequence: repetition time (TR) = 2000 ms; echo time (TE) = 30 ms; flip angle = 90°; acquisition matrix = 64 × 64; field of view (FOV) = 240 × 240 mm<sup>2</sup>; thickness = 5.0 mm, without gap; voxel size = 3.75 × 3.75 × 5 mm<sup>3</sup> and 205 volumes. During the 410-sec data acquisition period, the participants were instructed to keep their eyes closed, not think of anything in particular, and move as little as possible.

### Data preprocessing

Data preprocessing was performed using Statistical Parametric Mapping software (SPM8; [www.fil.ion.ucl.ac.uk/spm](http://www.fil.ion.ucl.ac.uk/spm)) and Data Processing Assistant for Resting-State fMRI (DPARSF) (Yan and Zang, 2010). First, we removed the first ten volumes and performed slice time correction and head motion correction. One healthy control subject with excessive head motion (above 3 mm or 3° in any direction) was excluded. Functional images were normalized to the EPI template in standard Montreal Neurological Institute (MNI) space provided in SPM8 with an optimum 12-parameter affine transformation and nonlinear deformations, resampled to 3-mm isotropic voxels, and spatially smoothed with a 4-mm full-width at a half-maximum Gaussian kernel. After removing linear trends and temporal band-pass filtering (0.01–0.1 Hz), Friston's twenty-four head motion parameters and three other confounding signals (white matter, cerebrospinal fluid and global signals) were regressed from the time course of each voxel.

### Network construction

A flow chart of the analysis strategy for the current study is illustrated in Fig. 1. Briefly, SAD-related brain networks for participants were constructed at the macroscale in which nodes represent brain regions and edges represent interregional functional connectivity. We selected SAD-

**Table 1**  
Demographics and clinical characteristics of study participants.

|                           | SAD (n = 33)     | HC (n = 32)    | p Value             |
|---------------------------|------------------|----------------|---------------------|
| Gender (Male/Female)      | 20/13            | 19/13          | 0.919 <sup>a</sup>  |
| Age (years)               | 18-38 (25 ± 6)   | 19-35 (25 ± 4) | 0.715 <sup>b</sup>  |
| Illness Onset Age (years) | 5-36 (18 ± 7)    |                |                     |
| Illness Duration (years)  | 1-20 (7 ± 4)     |                |                     |
| LSAS <sub>total</sub>     | 24-105 (61 ± 22) | 1-88 (35 ± 22) | <0.001 <sup>b</sup> |
| LSAS <sub>fear</sub>      | 13-55 (30 ± 11)  | 0-47 (16 ± 13) | <0.001 <sup>b</sup> |
| LSAS <sub>avoidance</sub> | 11-62 (30 ± 11)  | 0-45 (18 ± 11) | <0.001 <sup>b</sup> |

Data are presented as the range of minimum-maximum (mean ± SD).

SAD, social anxiety disorder; HC, health controls; LSAS<sub>total</sub>, LSAS<sub>fear</sub>, LSAS<sub>avoidance</sub>, total score and fear and avoidance subscales of the Liebowitz Social Anxiety Scale (LSAS).

<sup>a</sup> The p value was obtained using a chi-square test.

<sup>b</sup> The p value was obtained using a two-sample t-test.

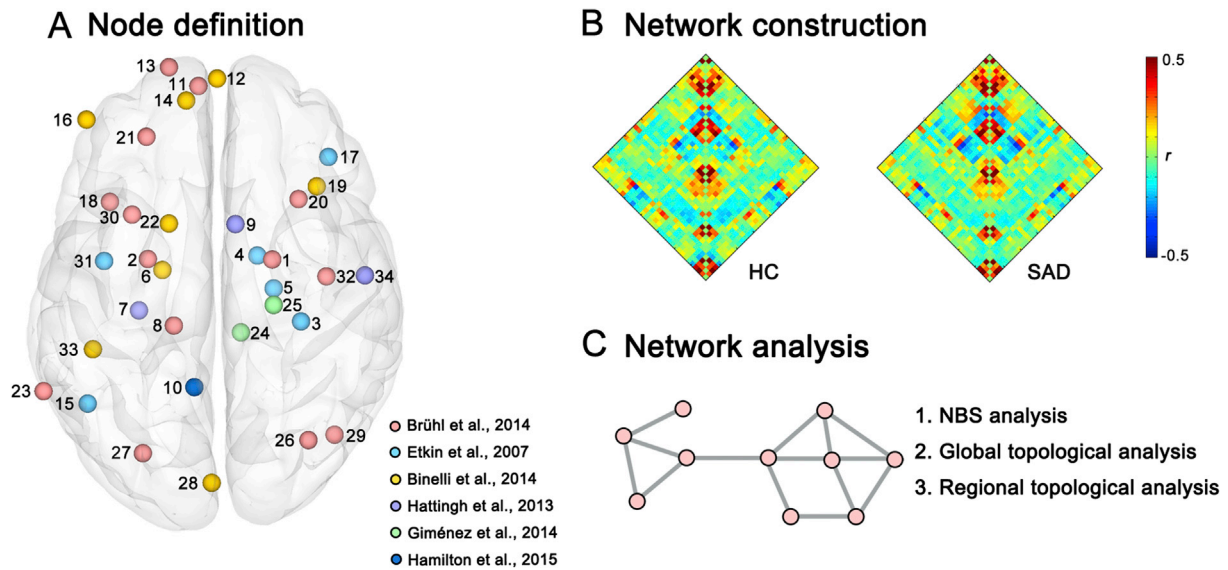


**Fig. 1. Flow chart of the network analysis of the SAD-related functional network using resting-state fMRI.** (A) Definition of nodes related to SAD. The ROI set was generated using prior studies (described in the manuscript) that identified a total of 34 nodes. (B) The matrices show the average functional network in both HC (left) and SAD (right). The edges in the network were defined as the Pearson correlation between any pair of nodes based on the resting-state time series. The color indicates the weight of each edge. (C) The abnormality of the SAD network was determined based on a network connectivity analysis using a network-based static (NBS) approach and a network topology analysis using global and regional topological metrics.

related network nodes (Fig. 1A and Table 2) by combining all previous meta-analyses involving abnormal brain activation during task performance in fMRI studies on SAD published before 2016 (Binelli et al., 2014;

Bruhl et al., 2014; Etkin and Wager, 2007; Hattingh et al., 2013) and two recent studies (Gimenez et al., 2014; Hamilton et al., 2015). Considering the important role of the thalamus and posterior cingulate cortex (PCC)

**Table 2**

Coordinates of thirty-four predefined regions of interest.

| ROI | Region                             | Abbreviations | BA | MNI Coordinate |     |     | Source |
|-----|------------------------------------|---------------|----|----------------|-----|-----|--------|
|     |                                    |               |    | X              | Y   | Z   |        |
| 1   | Right Amygdala                     | AMYG.R        | NA | 21             | -3  | -12 | a      |
| 2   | Left Amygdala                      | AMYG.L        | NA | -24            | -3  | -20 | a      |
| 3   | Right Fusiform gyrus               | FFG.R         | 20 | 32             | -26 | -28 | b      |
| 4   | Right Parahippocampal gyrus        | PHG.R         | 28 | 16             | -2  | -24 | b      |
| 5   | Right Parahippocampal gyrus        | PHG.R         | 36 | 22             | -14 | -26 | b      |
| 6   | Left Parahippocampal gyrus         | PHG.L         | 36 | -19            | -7  | -28 | c      |
| 7   | Left Parahippocampal gyrus         | PHG.L         | 30 | -27            | -22 | -24 | d      |
| 8   | Left Anterior cingulate gyrus      | ACC.L         | 23 | -14            | -28 | 42  | a      |
| 9   | Right Anterior cingulate gyrus     | ACC.R         | 24 | 8              | 9   | 35  | d      |
| 10  | Left Posterior cingulate gyrus     | PCC.L         | 23 | -7             | -50 | 28  | f      |
| 11  | Left Medial superior frontal gyrus | SFG.L         | 10 | -6             | 60  | 1   | a      |
| 12  | Left Medial superior frontal gyrus | SFG.L         | 10 | 1              | 63  | 30  | c      |
| 13  | Left superior frontal gyrus        | SFG.L         | 10 | -16            | 67  | 6   | a      |
| 14  | Left Medial orbitofrontal cortex   | ORB.L         | 11 | -10            | 55  | -10 | c      |
| 15  | Left Middle temporal gyrus         | MTG.L         | 37 | -46            | -56 | 10  | b      |
| 16  | Left Inferior frontal gyrus        | IFG.L         | 46 | -46            | 48  | 9   | c      |
| 17  | Right Inferior frontal gyrus       | IFG.R         | 45 | 42             | 34  | 4   | b      |
| 18  | Left Insula                        | INS.L         | 47 | -38            | 18  | -2  | a      |
| 19  | Right Insula                       | INS.R         | 47 | 38             | 23  | -3  | c      |
| 20  | Right Insula                       | INS.R         | 47 | 31             | 19  | -18 | a      |
| 21  | Left Middle frontal gyrus          | MFG.L         | 9  | -25            | 41  | 33  | a      |
| 22  | Left Putamen                       | PUT.L         | NA | -16            | 10  | -8  | c      |
| 23  | Left Supramarginal gyrus           | SMG.L         | 40 | -62            | -51 | 30  | a      |
| 24  | Thalamus                           | THA           | NA | 10             | -30 | 2   | e      |
| 25  | Thalamus                           | THA           | NA | 22             | -20 | 14  | e      |
| 26  | Right Inferior occipital gyrus     | IOG.R         | 19 | 35             | -69 | -6  | a      |
| 27  | Left Fusiform gyrus                | FFG.L         | 18 | -26            | -74 | -8  | a      |
| 28  | Left Calcarine sulcus              | CAL.L         | 18 | -1             | -85 | 13  | c      |
| 29  | Right Cerebellum                   | Cere.R        | NA | 44             | -67 | -20 | a      |
| 30  | Left Middle frontal gyrus          | MFG.L         | 44 | -30            | 13  | 39  | a      |
| 31  | Left Insula                        | INS.L         | 48 | -40            | -4  | 6   | b      |
| 32  | Right Insula                       | INS.R         | 48 | 41             | -10 | 12  | a      |
| 33  | Left Superior temporal gyrus       | STG.L         | 41 | -44            | -36 | 9   | c      |
| 34  | Right Rolandic operculum           | ROL.R         | 48 | 55             | -9  | 16  | d      |

The letter of source indicates the prior study establishing relevance of the region for SAD: a, Bruhl et al., 2014; b, Etkin and Wager, 2007; c, Binelli et al., 2014; d, Hattingh et al., 2013; e, Gimenez et al., 2014; f, Hamilton et al., 2015. L, left; R, right; BA, Brodmann area; NA, not available.

in SAD identified in many review articles, including R-fMRI studies, despite the lack of identification of these regions in prior meta-analyses (Engel et al., 2009; Fouche et al., 2013; Freitas-Ferrari et al., 2010; Marchand, 2010), we included these regions as well.

The location of maximal group difference in regions showing abnormality in SAD in each prior study or meta-analysis (Binelli et al., 2014; Bruhl et al., 2014; Etkin and Wager, 2007; Gimenez et al., 2014; Hamilton et al., 2015; Hattingh et al., 2013) was included in a collection of nodes with a 5-mm radius if they did not overlap with each other (thirteen overlapping nodes were identified and deleted). Thus, we considered multiple cortical and cerebellar regions, striatum, amygdala and thalamus as nodes (34 nodes in total, See Table 2). Next, we extracted the mean time series for each node. Interregional resting-state functional connectivity for each participant was evaluated by calculating the Pearson correlation between the time series of each node pair. Then, Fisher's  $r$ -to- $z$  transformation was applied to improve data distributions for parametric statistical analysis. Finally, the functional brain network based on previously identified SAD-related brain regions was obtained for each participant.

#### Network-based statistic (NBS) analysis

To identify the specific altered functional connectivity pattern in SAD, we utilized a NBS approach (Zalesky et al., 2010). This is a nonparametric method that controls the family-wise error rate when multiple test statistics are computed to evaluate connectivity disruption in a network. The NBS approach has been used to identify abnormal brain connectivity circuitry in depression (Bai et al., 2012; Zhang et al., 2011), schizophrenia (Zalesky et al., 2011), Alzheimer's disease (Wang et al., 2013) and attention-deficit/hyperactivity disorder (Cao et al., 2013).

Before the NBS analysis, to reduce spurious interregional connectivities, we first performed a one-sample  $t$ -test for each correlation within each group. Connectivities with corresponding  $p$  values that passed a significant non-zero threshold ( $p < 0.05$ , FDR-corrected) in each group were retained (the effect of network connectivity threshold was evaluated in a "Validation Analysis" discussed below). A union mask of significant connectivity was produced that included all connections that were significant in either of the two groups. This limited group comparisons to significant connectivity in at least one participant group. Then, within this mask, we performed two-sample  $t$ -tests to examine group differences in connectivity after controlling for age and gender. To avoid identifying a connectivity component that mixed increased and decreased connectivity together, we performed two-sample one-tailed  $t$ -tests (SAD > HC and SAD < HC, separately) for each connectivity estimate similar to previous studies (Bai et al., 2012; Cao et al., 2013; Wang et al., 2013; Zhang et al., 2011).

The subsequent NBS analysis was performed in three steps. First, a threshold ( $p < 0.05$ ) was applied to identify suprathreshold connections, among which any connected components and their size (the number of connections) were determined. Second, a nonparametric permutation approach was used to derive the empirical null distribution of connected component size for estimating the significance of each connected component (10,000 permutations). Briefly, in each permutation, all participants were randomly reallocated into two groups, and two-sample  $t$ -tests were recomputed as mentioned above. The same primary threshold ( $p < 0.05$ ) was used to produce suprathreshold connections among which the size of the maximal connected component was recorded. Finally, for a connected component of size  $N$  found in the real grouping of HC and patients, its corrected  $p$  value was determined by finding the proportion of the 10,000 permutations for which the maximal connected component was larger than  $N$ .

#### Graph-theory network analysis

Next, we explored topological network/nodal properties at both the global and regional levels in SAD patients compared to controls. For the

obtained functional brain networks, we calculated both global and regional topological metrics for each participant. The global network metrics included global efficiency ( $E_{glob}$ ), local efficiency ( $E_{loc}$ ), clustering coefficient ( $C_p$ ), shortest path length ( $L_p$ ), modularity ( $Q$ ) and small-world attributes ( $\gamma$ ,  $\lambda$  and  $\sigma$ ) (Danon et al., 2006; Latora and Marchiori, 2001; Onnela et al., 2005; Watts and Strogatz, 1998). For the regional network metrics, we evaluated nodal degree ( $D_{nodal}$ ), nodal efficiency ( $E_{nodal}$ ) and nodal participation coefficient ( $PC_{nodal}$ ) (Achard and Bullmore, 2007; Buckner et al., 2009; Liang et al., 2013; Liao et al., 2013, 2017). Briefly,  $E_{glob}$  measures the global efficiency of the parallel information transfer in the network and  $E_{loc}$  reveals the network fault tolerance level, which shows the communication efficiency among the first neighbors of a node when it is removed;  $C_p$  indicates the extent of local cliquishness in a network and  $L_p$  of the network quantifies the mean distance or routing efficiency between any pair of nodes;  $Q$  measures the difference between the proportion of intra-module links of an actual network and those of a random network; and small-world attributes indicate the degrees of small-world organization which reflects an optimal balance of integration and segregation for a network.  $D_{nodal}$  reflects the information communication ability,  $E_{nodal}$  characterizes the efficiency of the parallel information transfer, and  $PC_{nodal}$  measures the ability to integrate with other modules for a given node in the network. See "Supplementary Material" for formulas used to obtain these measurements.

Before calculating global and regional network metrics, we first binarized the network for each participant, to ensure nodes were connected independent from connectional weight. Considering that topological property computation has a strong dependency upon network density, we conservatively selected a large range of sparsity from 5% to 95% with a step of 5% instead of a single threshold to comprehensively estimate topological properties covering a wide range of sparsity. In the binarization, for a given sparsity threshold  $n\%$ , the strongest connections with the highest  $n\%$  absolute value in the network were set to 1, and the other connections were set to 0. Finally, we computed the area under the curve (AUC) for each global/regional metric to provide a summary measure for topological organization independent from any single threshold selection. All network analyses in this study were performed using the GREYNA toolbox (Wang et al., 2015) (<http://www.nitrc.org/projects/greyna/>), and the results were visualized using the BrainNet Viewer (Xia et al., 2013) (<http://www.nitrc.org/projects/bnv/>).

To detect group differences between SAD and HC in AUC values for each network metric, we used a general linear model with each global/regional network metric as the dependent variable, subject group as the independent variable, and age and gender as covariates. For multiple comparisons of regional network metrics, we used two different correction approaches. First, as a preliminary exploration, we used a less strict false-positive correction for the multiple comparisons (thirty-four regions) of each nodal property,  $1/N = 0.029$ , where  $N$  is the number of comparisons, which implies less than 1 false positive per analysis on average (Fornito et al., 2011; Lynall et al., 2010). Second, we performed Bonferroni correction as a strict approach for the multiple comparison correction for analysis of nodal properties. In addition, we calculated Cohen's  $d$  (Cohen, 1988) to estimate the effect size of significant results. For those connectivity components or topological metrics with significant group differences between SAD and HC, we examined their relationship with current state clinical anxiety (i.e., LSAS) in the SAD group using partial correlation, with age and gender as covariates.

#### Validation analysis

To validate the robustness of our results, we examined the influence of different image preprocessing and data analysis strategies as follows.

- i) **Network connectivity threshold.** To determine whether our major results were dependent on the choices of connectivity thresholds (i.e.,  $p < 0.05$  FDR-corrected) in detecting abnormal

- functional connectivity components in SAD, we re-performed the NBS analysis using two other thresholds (i.e.,  $p < 0.01$  FDR-corrected and  $p < 0.001$  uncorrected).
- ii) **Network type effects.** Although binary networks reduced identification of disturbances in functional connectivity strength due to noise, the weight of connections may provide additional information to characterize the brain connectome. Therefore, we also implemented weighted network analyses to estimate the similarity of results between weighted and binary network analysis.
- iii) **Head motion.** First, we excluded one participant (a HC) with large head motion. We conducted further analysis to rule out potential effects of head motion that might confound estimation of functional connectivity by performing a ‘scrubbing’ procedure (Power et al., 2012) on the preprocessed images. For the volumes with a frame-wise displacement (FD) from the prior volume exceeding a threshold of 0.5 mm, we replaced the volumes and their adjacent volumes (2 forward and 1 backward frames) with nearest neighbor interpolated data within the fMRI time series of each participant (No volume with  $FD > 0.5$  was at beginning or end of scanning in our data). We then re-identified the disrupted NBS component and disrupted global and nodal topological property in SAD using the scrubbed R-fMRI data.
- iv) **Global signal.** Previous research has suggested that global signals are related to non-neuronal activity, such as respiration, and should therefore be removed (Birn et al., 2006; Fox et al., 2009). However, this processing also introduces a widespread negative functional connectivity and may alter the intrinsic connection architecture of brain networks (Murphy et al., 2009; Weissenbacher et al., 2009). Recently, Murphy and Fox (2016) suggested that preprocessing strategies with and without global signal regression may provide complementary insights into the

functional organization of the brain. Thus, we repeated our network analysis without global signal regression.

- v) **Network density.** The selection of optimal sparsity is still an open question in brain network analysis without any gold standard. In this study, we conservatively selected a large range of sparsity from 5% to 95% without priori assumptions about network density. Given concern about the balance between efficiency and cost of the topological organization might be broken in extremely densely connected networks, we repeated our network analysis using a shorter range of sparsity from 5% to 80%.

## Results

### Disrupted network connectivity in SAD

There was no significant group difference in mean functional connectivity estimates within the ‘a priori’ SAD network ( $p = 0.549$ ). However, NBS analysis revealed a single connected component with 31 nodes and 36 connections that showed higher functional connectivity ( $p = 0.002$  corrected, mean Cohen’s  $d = 0.58$ ) in SAD. Heightened connectivities within this single component were mainly located in the frontolimbic circuit, which includes the VMPFC, DLPFC, and limbic regions, and also occipital and parietal regions (Fig. 2A and Table S1). These findings suggest that frontolimbic and sensory/perceptual processing regions had increased resting brain connectivity, and that their increased connectivities were associated with each other as part of a single, integrated abnormal brain circuitry in SAD.

### Disrupted global and nodal topological properties in SAD

For the whole SAD-related network, both SAD and HC exhibited many typical features of small-world organization (Table S2). Nevertheless, compared with HC, the SAD had significantly lower AUC values of  $\lambda$

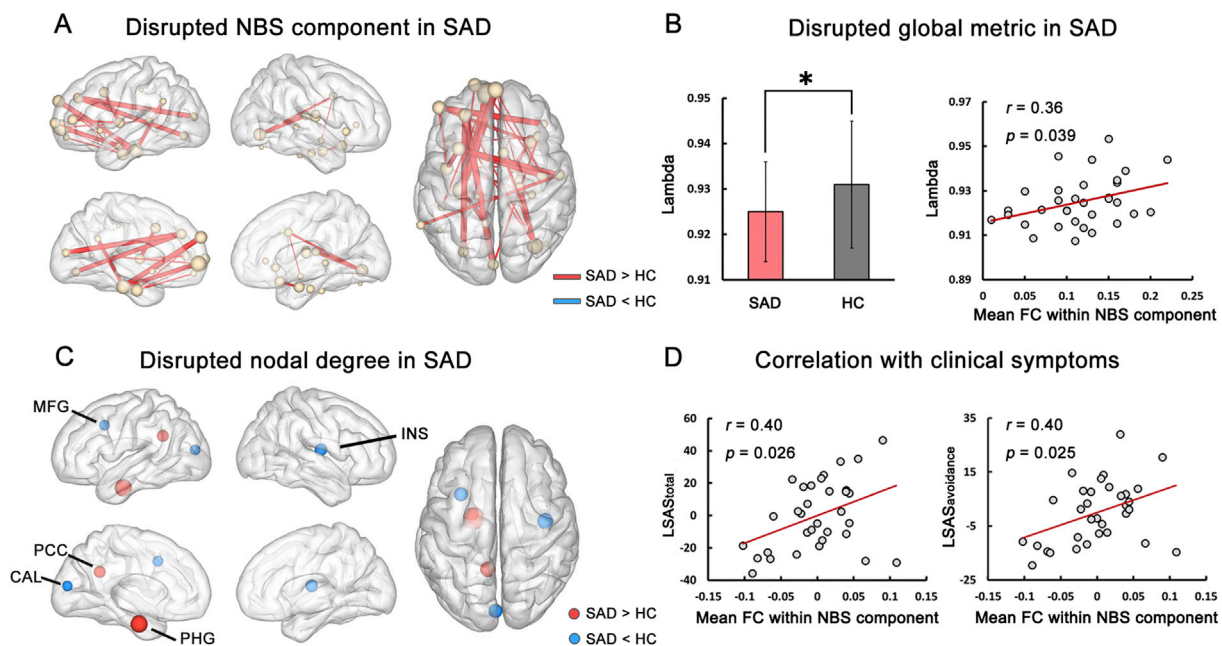


**Fig. 2. Network analysis and correlation with clinical variables.** (A) A single integrated SAD-related network component had higher functional connectivity in SAD than HC in an NBS analysis. The size of a node represents its number of functional connections. The size of an edge represents its altered degree of functional connectivity. (B) The histogram shows the global metric with significant differences between SAD and HC, and the scatter plot shows a positive correlation between the altered global metric and averaged FC within the SAD-related NBS component.  $*p < 0.05$ . (C) Abnormalities in nodal degree were revealed by regional topological analysis. The red nodes represent the regions showing an abnormally high nodal degree in SAD, and the blue nodes represent regions showing lower nodal degree in SAD compared with HC. The size of a node indicates the degree of group difference ( $t$  value). All regions listed passed a false-positive correction for the multiple comparisons; only left parahippocampal gyrus survived Bonferroni correction. (D) The scatter plots show positive correlations between the averaged FC within the SAD-related NBS component and self-reported social anxiety in the SAD group. Each dot represents data from one patient after we controlled for the effects of age and gender. SAD, social anxiety disorder; HC, healthy controls; MFG, middle frontal gyrus; PHG, parahippocampal gyrus; PCC, posterior cingulate cortex; CAL, calcarine sulcus; INS, insula; FC, functional connectivity; NBS, network-based statistic analysis; LSAS, Liebowitz Social Anxiety Scale.

( $p = 0.042$ , Cohen's  $d = -0.52$ ) in the SAD-related network (Fig. 2B, left), which suggests a relatively randomized global topology in SAD. Further, we found a positive correlation between this disrupted global property (AUC values of  $\lambda$ ) and the mean strength of the abnormal connectivity component that was revealed by the abovementioned NBS analysis ( $r = 0.36$ ,  $p = 0.039$ ) (Fig. 2B, right). This result suggests that deficits in global topology in SAD may be caused in part by abnormally high connectivity in the network. There were no significant differences in other global topological metrics (Table S2).

Regional topological analysis (Fig. 2C, Table 3 and Table S3) showed that the nodal degree, efficiency and participation coefficient in left parahippocampus and PCC were larger in SAD than HC. Follow-up analysis revealed that these two regions had become abnormal hub regions in the SAD-related network (See Table 4, the definition of hubs was based on the nodal degree in the group-averaged network for each group). Moreover, SAD had less nodal degree and efficiency in the right insula, left calcarine sulcus and the middle frontal gyrus, and less nodal participation coefficient in the left calcarine sulcus than HC. Together, these results indicate a disorganization of the global and regional topological properties in SAD.

#### Relationship between connectivity/topological metrics and clinical symptoms

In exploratory analyses, we found modest evidence for relationships between self-reported anxiety and functional connectivity indices. The mean strength of the significant connectivity component revealed by NBS analysis was positively correlated with the LSAS<sub>total</sub> ( $r = 0.40$ ,  $p = 0.026$ ) and LSAS<sub>avoidance</sub> scores ( $r = 0.40$ ,  $p = 0.025$ ) (Fig. 2D). No significant correlations were found between any topological metrics and SAD symptoms.

#### Robustness of findings

The findings reported above were generally stable across different network connectivity thresholds, network type, network density and preprocessing strategies (Fig. 3 and Table S4).

- i) **Network connectivity threshold.** Under different network connectivity thresholds, we observed a significant component (all  $p < 0.023$ ) with high functional connectivity in SAD in NBS analysis (the first two columns in Fig. 3A), which are very similar to our main results in Fig. 2A.
- ii) **Network type effects.** There were no significant group differences in the global topological metrics for the weighted network, which indicates that the weight of functional connectivity may influence the detection of abnormalities in the topological architecture of the SAD-related network. Regional topological analysis demonstrated the larger nodal degree and efficiency in left parahippocampus and lower nodal degree and efficiency in the right insula and left middle frontal gyrus in SAD than in HC (the second column of Table S4). In addition, there was a trend toward

**Table 4**  
The AUC value of nodal degree in SAD and HC groups.

| ROI | Regions | SAD                 | HC                  |
|-----|---------|---------------------|---------------------|
| 10  | PCC.L   | <b>17.10 ± 2.14</b> | 15.44 ± 3.04        |
| 31  | INS.L   | <b>16.68 ± 1.37</b> | <b>17.38 ± 1.93</b> |
| 18  | INS.L   | <b>16.66 ± 2.04</b> | <b>16.86 ± 2.18</b> |
| 6   | PHG.L   | <b>16.39 ± 1.84</b> | 14.33 ± 2.48        |
| 14  | ORB.L   | <b>16.22 ± 2.41</b> | 15.75 ± 2.37        |
| 12  | SFG.L   | <b>16.11 ± 2.69</b> | <b>15.89 ± 2.42</b> |
| 19  | INS.R   | <b>16.06 ± 2.46</b> | <b>16.44 ± 2.37</b> |
| 11  | SFG.L   | 15.97 ± 2.11        | <b>16.06 ± 2.10</b> |
| 9   | ACC.R   | 15.79 ± 2.47        | 14.91 ± 2.20        |
| 5   | PHG.R   | 15.72 ± 2.41        | 15.11 ± 2.39        |
| 7   | PHG.L   | 15.59 ± 2.46        | 14.38 ± 2.35        |
| 2   | AMYG.L  | 15.44 ± 2.06        | 14.71 ± 2.65        |
| 17  | IFG.R   | 15.43 ± 2.06        | <b>16.18 ± 2.39</b> |
| 34  | ROL.R   | 14.91 ± 2.28        | 15.85 ± 2.02        |
| 8   | ACC.L   | 14.76 ± 2.08        | 14.09 ± 2.64        |
| 3   | FFG.R   | 14.75 ± 2.01        | 13.96 ± 2.53        |
| 13  | SFG.L   | 14.75 ± 2.61        | 14.57 ± 2.58        |
| 16  | IFG.L   | 14.71 ± 2.23        | 13.50 ± 2.10        |
| 23  | SMG.L   | 14.66 ± 2.25        | 14.49 ± 2.78        |
| 15  | MTG.L   | 14.65 ± 2.21        | 13.68 ± 2.67        |
| 20  | INS.R   | 14.64 ± 2.44        | 15.02 ± 2.09        |
| 27  | FFG.L   | 14.58 ± 2.16        | 14.84 ± 2.77        |
| 4   | PHG.R   | 14.52 ± 2.07        | 14.57 ± 2.26        |
| 32  | INS.R   | 14.31 ± 2.04        | 15.83 ± 2.37        |
| 22  | PUT.L   | 14.24 ± 2.41        | 14.42 ± 2.36        |
| 21  | MFG.L   | 14.19 ± 2.33        | 15.21 ± 2.38        |
| 1   | AMYG.R  | 13.93 ± 2.19        | 14.54 ± 2.78        |
| 29  | Cere.R  | 13.90 ± 2.20        | 14.49 ± 2.81        |
| 33  | STG.L   | 13.68 ± 2.21        | 14.21 ± 2.01        |
| 24  | THA     | 13.67 ± 2.21        | 13.28 ± 2.69        |
| 28  | CAL.L   | 13.38 ± 2.46        | 14.66 ± 1.90        |
| 26  | IOG.R   | 12.98 ± 2.49        | 13.55 ± 2.57        |
| 30  | MFG.L   | 12.94 ± 2.30        | 14.27 ± 2.24        |
| 25  | THA     | 12.51 ± 2.86        | 13.36 ± 2.16        |

Data are presented as the mean ± SD.

Hubs (above 1 SD) in each group are shown in boldface. Definition of hubs was based on degree centrality for each node in the average network for each group.

significance in the left calcarine sulcus with lower nodal degree and efficiency in SAD. The majority of the results in the graph-theory topological network analysis survived.

- iii) **Head motion.** There was no significant difference ( $p = 0.746$ ) between the mean FD value of the HC group ( $0.24 ± 0.13$ ) and the SAD group ( $0.23 ± 0.13$ ), and 94% of the participants had a mean FD less than 0.5 mm. The average percentage of volume with FD above 0.5 mm was 7% in both the HC and SAD groups. Using the scrubbed R-fMRI data, we found a significantly higher functional connectivity component ( $p = 0.001$ ) (the third column in Fig. 3A) and disrupted global and nodal topological properties in SAD (the third column of Table S4). Briefly, the abnormal component included the ventromedial and dorsolateral prefrontal, limbic, occipital and parietal regions, which are almost identical to findings in our primary analyses. We also found that SAD had larger nodal degree and efficiency in the left parahippocampus and posterior cingulate cortex but had lower nodal degree and

**Table 3**  
Brain regions with significant group difference in nodal degree, efficiency and participation coefficient.

| Regions            | $D_{\text{nodal}}$ |              | $t$   | $p$     | $E_{\text{nodal}}$ |             | $t$   | $p$     | $PC_{\text{nodal}}$ |             | $t$   | $p$   |
|--------------------|--------------------|--------------|-------|---------|--------------------|-------------|-------|---------|---------------------|-------------|-------|-------|
|                    | SAD                | HC           |       |         | SAD                | HC          |       |         | SAD                 | HC          |       |       |
| <b>SAD &gt; HC</b> |                    |              |       |         |                    |             |       |         |                     |             |       |       |
| PHG.L              | 16.39 ± 1.84       | 14.33 ± 2.48 | 3.71  | <0.001* | 0.67 ± 0.03        | 0.63 ± 0.05 | 3.77  | <0.001* | 0.73 ± 0.07         | 0.68 ± 0.07 | 2.69  | 0.009 |
| PCC.L              | 17.10 ± 2.14       | 15.44 ± 3.04 | 2.55  | 0.013   | 0.68 ± 0.04        | 0.65 ± 0.06 | 2.61  | 0.012   | 0.75 ± 0.05         | 0.71 ± 0.07 | 2.66  | 0.010 |
| <b>SAD &lt; HC</b> |                    |              |       |         |                    |             |       |         |                     |             |       |       |
| INS.R              | 14.31 ± 2.28       | 15.83 ± 2.38 | -2.68 | 0.009   | 0.63 ± 0.04        | 0.66 ± 0.04 | -2.55 | 0.013   |                     |             |       |       |
| CAL.L              | 13.38 ± 2.46       | 14.66 ± 1.90 | -2.30 | 0.025   | 0.60 ± 0.06        | 0.63 ± 0.04 | -2.38 | 0.020   | 0.66 ± 0.08         | 0.71 ± 0.06 | -2.57 | 0.013 |
| MFG.L              | 12.94 ± 2.30       | 14.27 ± 2.24 | -2.27 | 0.027   | 0.60 ± 0.06        | 0.63 ± 0.05 | -2.30 | 0.025   |                     |             |       |       |

The values of  $D_{\text{nodal}}$ ,  $E_{\text{nodal}}$ , and  $PC_{\text{nodal}}$  represent the AUC values (mean ± SD) of the nodal degree, nodal efficiency and nodal participation coefficient of SAD and HC group.

\* $p < 0.05$  Bonferroni corrected. L, left; R, right; SAD, social anxiety disorder; HC, healthy control.

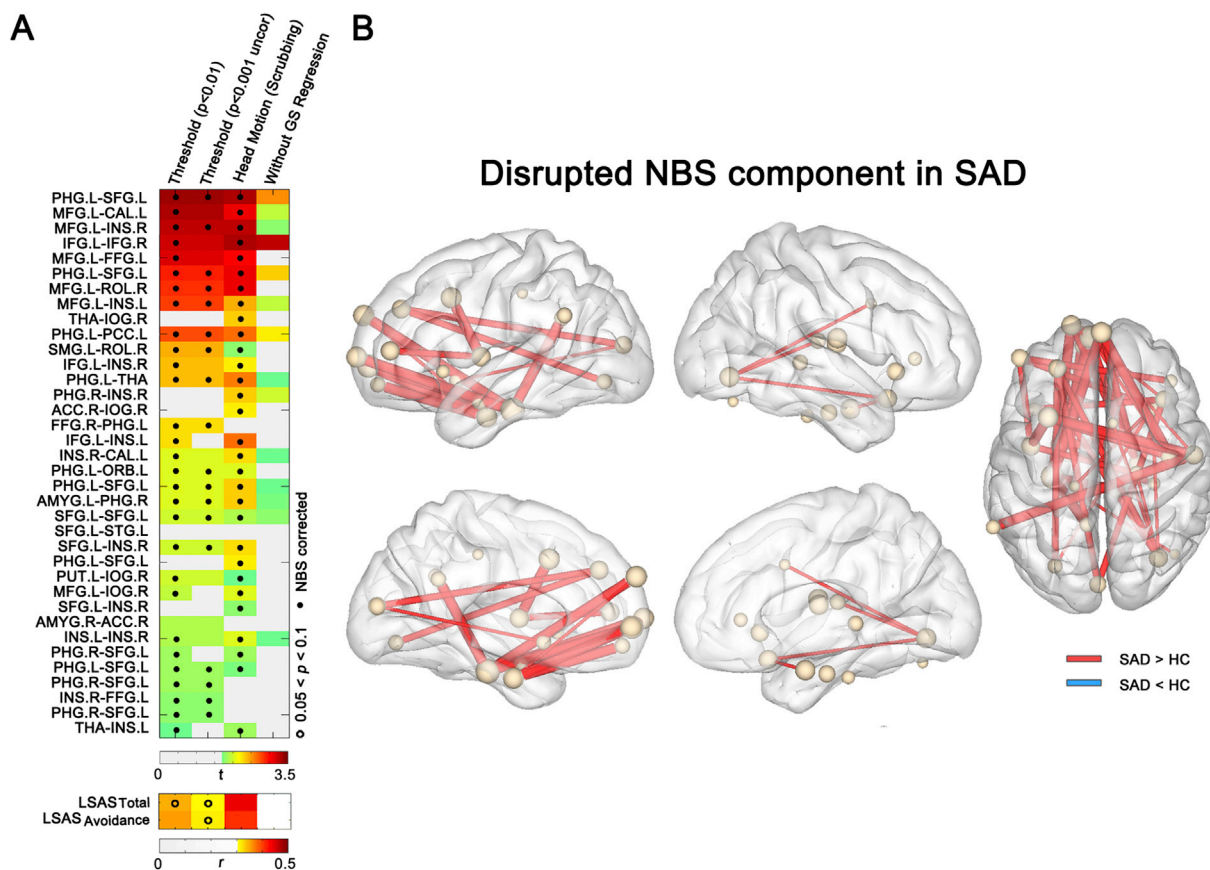


**Fig. 3.** The results of the NBS analysis and their correlation with clinical variables in a validation analysis. (A) The color in the top matrix represents the  $t$  value for network connectivity. Only network connectivities with  $p < 0.05$  are shown in the matrix. Each column represents the result of different preprocessing or analysis strategies. The solid circle indicates the network connectivity indices that are significant in the NBS analysis with correction for multiple comparison. The color in the bottom matrix represents the  $r$  value of the correlation between mean strength within the NBS component and LSAS anxiety scores. To fully describe the pattern of effects across approaches, a hollow circle is also shown to indicate a trend toward a significant effect ( $p < 0.1$ ). (B) The brain map shows the significantly higher functional connectivity in SAD than HC in the NBS analysis across different image processing strategies. The size of a node represents the total number of its functional connectivities. The size of an edge represents the frequency of occurrence for each functional connectivity across different image processing strategies. GS, global signal.

efficiency in the right insula and left calcarine sulcus than HC. Moreover, there was a trend toward lower AUC values of  $\lambda$  in SAD ( $p = 0.080$ ).

- iv) **Global signal.** The result of the NBS analysis using preprocessing data without global signal regression is shown in Fig. 3A (the last column) and only part of the functional connectivity within the NBS component seen in findings from primary analyses survived under a threshold of  $p < 0.05$  uncorrected. No significant differences were found in the global and nodal topological properties. To exclude the possibility that global signal regression introduced a bias into the data and lead to the observations in our main results, we further calculated the amplitude of low-frequency fluctuations (ALFF) of global signal for each participant and examined its group differences. No significant difference was found in the global signals between the SAD and HC groups ( $p < 0.409$ ). Thus, preprocessing without global signal regression reduced detection of connectional and topological disturbances in SAD (see the last column of Fig. 3A and the fourth column of Table S4), probably because global signal levels can be associated with mechanical or non-neuronal factors during image acquisition (Birn et al., 2006).
- v) **Network density.** With a connection density range of 5%–80%, we observed highly similar results to those reported from our primary analyses on the AUC values of global and nodal topological properties across density range (the last column of Table S4).

Finally, we combined all results in the NBS analysis across different

preprocessing and analysis strategies, and the conjunction map of the component is shown in Fig. 3B, which shows that most of our results were stable.

## Discussion

Using R-fMRI and graph-theory network analysis, we identified a widespread network-level pathophysiological profile in SAD in terms of both connectivity patterns and topological metrics. Importantly, the study sample was treatment naïve to ensure that the findings were not confounded by drug or psychotherapeutic interventions. Three main findings emerged from this study. First, the NBS analysis revealed that patients with SAD exhibited a single abnormal connectivity component in a circuit involving both frontolimbic (VMPFC, DLPFC, and insula) and sensory and perceptual processing regions (occipital and PCC). Connectivity was altered within and between these two brain circuits. Thus, abnormalities in these circuits are related and are not independent. Second, the graph-theoretical analysis demonstrated a lower normalized characteristic path length and altered nodal centralities of SAD-related neural circuitry in the SAD group. Moreover, aberrant connectivity was associated with acute symptom severity. Thus, resting brain connectivity impairments are clinically relevant due to their linkage with emotional disturbances seen in SAD. While some of these impairments have been previously observed during task-based fMRI studies, our findings indicate that abnormalities in these regions are also seen in resting brain physiology. Thus, the persistent social anxiety and associated neural hyperexcitability during social situations associated with SAD may induce or

result from altered resting brain physiology in ways that lead to both alterations in task-based activation and persistent illness.

#### Network connectivity dysfunction in SAD

At the network connectivity level, we observed SAD-associated pathologically increased functional connectivity in frontolimbic circuitry and the occipital and posterior cingulate cortices. Although widely distributed functional dysconnectivity in the frontolimbic, parietal and occipital regions have been demonstrated in previous R-fMRI studies (Arnold Anteraper et al., 2014; Ding et al., 2011; Hahn et al., 2011; Liao et al., 2010), the dysconnectivity within these regions has been largely considered to represent independent abnormalities in isolation from each other. The R-fMRI network analysis based on graph theory allowed us to reveal the intrinsic network-level dysfunction in SAD.

Summarizing our findings from the perspective of connectivity, we propose a network-level neurobiological model based on our results (Fig. 4). In the frontolimbic circuit that supports emotion regulation, we found increased functional connectivity between the DLPFC, VMPFC and limbic regions. Connections within the frontolimbic circuitry have been suggested to integrate “top-down” cognitive control of activity within brain regions associated with emotion processing, and abnormalities in this circuitry can lead to clinical features such as anxiety and fear (Pavuluri et al., 2005). Reduced connectivity can reflect reduced top-down modulation of emotion, and increased connectivity can reflect increased efforts at emotion regulation which can be variably successful. Hypoactivation in the prefrontal cortex and hyperactivation in limbic regions have been previously reported in task-based fMRI research (Gross and Hen, 2004; Guyer et al., 2008; Klumpp et al., 2012), which has been interpreted to reflect the failure of top-down inhibition mechanisms to reduce the intensity and duration of anxiety in SAD. To modulate exaggerated emotional reactivity, cognitive control mechanisms and emotion regulation are required.

However, from a connectivity analysis perspective, rather than being decreased, our data indicate that connectivity is increased in the frontolimbic/perceptual system circuit. The disrupted functional connectivity pattern involved a series of interconnected connectivities as part of a single abnormal component in patients. In the current study, we used an NBS analysis that identifies differences between groups by exploiting interconnected nodes with a deviant connectivity pattern (subnetworks) and provides information about topology of complex networks associated with the effect of interest (Zalesky et al., 2010). From a network perspective, the increased connectivity pattern observed in the current study can be seen as increased coupling and integrated communication within a set of interconnected regions, rather than isolated abnormalities in local nodes. An appealing interpretation of this finding is that top-down control modulation is increased but still fails to compensate for heightened social anxiety. This interpretation is consistent with the observation that the DLPFC and cingulate regions show positive connectivity with the amygdala (Etkin et al., 2011), and with the observation of the amygdala-DLPFC coupling during the processing of fearful faces in healthy subjects (Robinson et al., 2012). These findings suggest that frontolimbic circuitry is enhanced in a potentially compensatory manner but still fails to modulate emotion in SAD. This failure of top-down emotion modulation may represent one neural mechanism contributing to debilitating social anxiety associated with the disorder.

In the domain of perception and attention, SAD-associated network deficits involved heightened functional connectivity at rest between frontolimbic and PCC/occipital regions. It is well documented that SAD may arise from abnormalities in cortical/subcortical interactions, resulting in inappropriate expression of fear responses and hypervigilance toward social stimuli (Gentili et al., 2008). Previous studies have reported altered activations in VMPFC and visual areas in SAD when patients respond to social threat and scrutiny (Gentili et al., 2008; McClure et al., 2007), which potentially arise from an attempt to exert inhibitory modulation of emotional responses and internal processing of

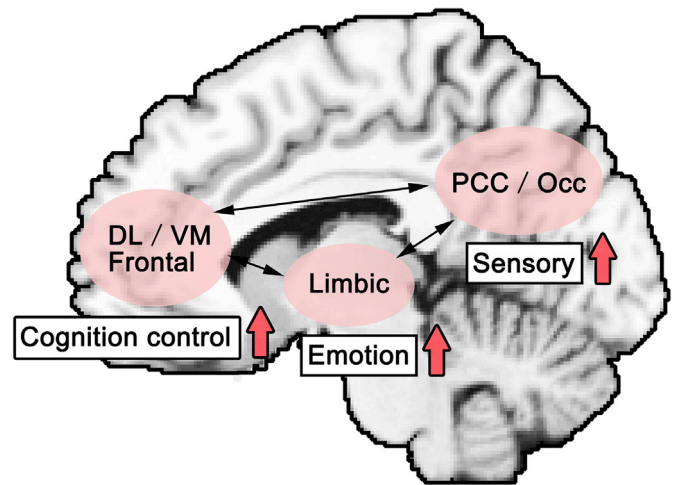


Fig. 4. A network model of the dysfunctional brain connectome in SAD. (A) Within the circuit of emotion regulation, the increased connection between the DL/VMPFC and limbic regions is believed to reflect the presence of increased activity in the cognitive control system over the emotion system in the brain. This increase may provide some compensatory if not fully effective reduction in illness severity. (B) In the domain of perception and attention, heightened connections between the frontal and PCC/occipital regions and those between the limbic and visual regions, may represent an effort at top-down control of perceptual activity and a heightened emotional influence on perceptual processing, respectively in SAD. DL/VMPFC, dorsolateral/ventromedial prefrontal cortex; PCC, posterior cingulate cortex; Occ, occipital cortex.

emotional visual images. A recent meta-analysis highlighted robust abnormalities in parietal and medial occipital regions in SAD (Bruhl et al., 2014), which have often been neglected in previous pathological models. Disrupted topological organization in these regions was apparent in our data as well. The increased connection between sensory processing areas and frontolimbic regions could result from an increased concern about social threat leading to both an ongoing heightened attentiveness to sensory input and perceptual analysis of sensory events in SAD (Bruhl et al., 2011; Sylvester et al., 2012).

One of the key symptoms in SAD is a persistent and debilitating focus upon negative or potentially threatening stimuli. This overactive processing of sensory events is seen clinically as a hypervigilance to social stimuli, exaggerated fear responses and increased avoidance behavior. The increased vigilance regarding social cues may thus be reflected in abnormal fronto-occipital connectivity. Importantly, this increased connectivity pattern in our study correlated with social avoidance and fear symptoms in SAD, which supports the hypothesis that hypervigilance to threat cues in SAD can be seen at the neural, psychological, and behavioral levels.

#### Global and regional topological disorganization of functional networks in SAD

With regard to the disrupted topological properties in the SAD-related network, at the global level, SAD was associated with a more randomized functional neural network organization. Compared with small-world networks, random networks have less modularized information processing and fault tolerance (Latora and Marchiori, 2001). Although the biological mechanism underlying this shift remains to be determined, a shift toward randomization is generally associated with increased signal propagation speed and synchronizability (Strogatz, 2001). In this study, we observed a correlation between relative randomization and abnormally increased functional brain connectivity in SAD.

At the regional level, the unusually large nodal centralities in SAD were most apparent in the parahippocampal gyrus and PCC/precuneus. These regions are key parts of the default-mode network (DMN) that are

typically involved in self-focused attention (Brewer et al., 2013). The parahippocampal gyrus and the amygdala-entorhinal pathway play vital roles in the integration of threat information and the orchestration of inhibition of emotional response expression through synchronized activity with distant brain regions (Majak and Pitkanen, 2003). Thus, our observations of large nodal centralities in the PCC and parahippocampal cortex may represent a neural substrate of the abnormally elevated stimulus-driven attention and emotional responses that characterize SAD. In addition, the hub regions identified in the disease-related network in SAD partially overlapped with hubs identified in the whole brain networks (e.g., PCC/precuneus and insula), which were reported in a previous study (Liu et al., 2015). Nevertheless, the abnormality in the PCC/precuneus was increased in our study but decreased in the data reported by Liu et al. (2015), which may be due to the definitions of hubs in terms of different types of networks (disease-related vs. whole brain). In this case, network analysis at different levels (focusing disease-related regions or whole brain) may provide complementary insights into the abnormal neural mechanisms in SAD.

Low nodal centralities in SAD were mainly seen in the dorsolateral prefrontal, insular and calcarine cortex. Evidence from task-based functional imaging studies has shown that pathological anxiety is associated with hypoactivity in the dorsolateral prefrontal cortex (Klumpff et al., 2010; Pujol et al., 2013), which is presumably related to deficiencies in cognitive control over emotional responses to anxiety-provoking events. Similarly, lower ALFF in the insular node (Zhang et al., 2015) and decreased connectivity between the insula and cingulate cortex (Klumpff et al., 2012) have been reported in SAD. Although several studies have reported exaggerated visual responses in SAD (Frick et al., 2013, 2014), others have failed to find visual hyperactivity or even found a decreased occipital response (Binelli et al., 2015; Gentili et al., 2008). This discrepancy may indicate the complicated visual processing pattern, which includes both increased vigilance and stimulus avoidance in SAD, psychiatric treatment effects, or the complex interplay between increased sensory responsivity with variable and perhaps inconstant top-down modulation of sensory responses.

In our study, patients with SAD showed significantly decreased centralities in nodal metrics, which were coupled with an increased connection in the NBS results. Nodal degree is a local nodal measure evaluating the connection between a node and all other nodes in a network (Achard and Bullmore, 2007). As such, reduced nodal degree with increased functional connectivity in the NBS in these regions suggests that increased connectivity in the frontolimbic and occipital circuits is associated with reduced connections of these regions to other brain regions in the whole SAD network.

Clinically, the group difference of brain networks between individuals with SAD and HC identified in the current study provides further mechanistic understanding of this disorder from a connectomic perspective. Additionally, the present study adds to the developing psychoradiology (Lui et al., 2016), a new field of radiology, which seems primed to play a major clinical role in guiding diagnostic and treatment planning decisions in patients with psychiatric disorders. Future studies are necessary to clarify the potential value of our findings as biomarkers for clinical application, however our findings represent a positive step to support such advances.

#### Limitations and further considerations

Several limitations in the present study need to be considered. First, while our study establishes abnormalities in resting brain physiology in SAD, the relationship between our observations and the altered stimulus-driven responses in task-based fMRI or psychophysiological studies need to be examined to understand the relationship between abnormalities in resting and evoked neural system physiology. Second, since the sample was treatment naïve which is difficult to recruit in larger numbers, the sample size is moderate in our study. Further work with large sample size is needed to determine whether different clinical treatments (e.g.,

cognitive training, pharmacological treatments, TMS) can ameliorate the identified abnormalities in brain connectivity associated with SAD. Third, longitudinal studies are needed to determine whether there is a progressive change in the neural system alterations in SAD, with perhaps progressively enhanced evoked responses leading to greater resting physiology alterations (or the reverse). Such efforts will provide important insights into the pathophysiological mechanisms and course of illness of SAD that may lead to more personalized and effective therapies. Fourth, to explore the potential effect of anxiety during MR scans on functional connectivity, future MRI research in SAD may benefit from with recording of psychological responses and psychophysiological reactions of participants during or immediately before and after imaging studies. Finally, multimodal psychoradiological studies in the future may aid our developing understanding of SAD.

#### Conclusion

This is the first study to characterize abnormalities in resting brain physiology associated with severe social anxiety using R-fMRI and graph-theory network analysis. We identified a single aberrant connectivity component involving an integrated pattern of abnormalities in frontolimbic and PCC/occipital cortices, which were, to a moderate degree, correlated with the severity of social anxiety. From a network topological perspective, SAD was associated with a shift of topology toward randomized configuration together with a disorganization of regional topological properties. This less-optimized topological configuration might underlie the persistent cognitive and emotional deficits in SAD. In particular, this study adds to psychoradiology, a promising subspecialty for clinical radiology focusing on psychiatric disorders.

#### Conflicts of interest

Dr. Sweeney has consulted to Takeda Pharmaceuticals. Other authors have no conflicts to report.

#### Acknowledgments

We thank Xindi Wang for his help with data analyses. This study was supported by the National Natural Science Foundation (Grant Nos. 31700964, 81621003, 81220108013, 81227002, 81030027, 91432115, 81401479, 81671767 and 81620108016), the China Postdoctoral Science Foundation (Grant No. 2015M572479), Beijing Natural Science Foundation (Grant No. Z151100003915082), Beijing Brain Project (Grant No. Z161100000216125), Program for Changjiang Scholars and Innovative Research Team in University (PCSIRT, Grant No. IRT16R52) of China, Changjiang Scholar Professorship Award (Award Nos. T2014190 and T2015027) and the Fundamental Research Funds for the Central Universities (Grant Nos. 2017XTCX04 and 2015KJJA13). Dr. Sweeney acknowledges support from the Humboldt Foundation. Dr. Gong would also like to acknowledge the support from the American CMB Distinguished Professorship Award (Award No. F510000/G16916411) administered by the Institute of International Education, USA.

#### Appendix A. Supplementary data

Supplementary data related to this article can be found at <https://doi.org/10.1016/j.neuroimage.2017.12.011>.

#### References

- Achard, S., Bullmore, E., 2007. Efficiency and cost of economical brain functional networks. *PLoS Comput. Biol.* 3, e17.
- Arnold Anteraper, S., Triantafyllou, C., Sawyer, A.T., Hofmann, S.G., Gabrieli, J.D., Whitfield-Gabrieli, S., 2014. Hyper-connectivity of subcortical resting-state networks in social anxiety disorder. *Brain Connect.* 4, 81–90.
- Bai, F., Shu, N., Yuan, Y., Shi, Y., Yu, H., Wu, D., Wang, J., Xia, M., He, Y., Zhang, Z., 2012. Topologically convergent and divergent structural connectivity patterns

- between patients with remitted geriatric depression and amnesic mild cognitive impairment. *J. Neurosci.* 32, 4307–4318.
- Baker, S.L., Heinrichs, N., Kim, H.J., Hofmann, S.G., 2002. The Liebowitz social anxiety scale as a self-report instrument: a preliminary psychometric analysis. *Behav. Res. Ther.* 40, 701–715.
- Binelli, C., Muniz, A., Subira, S., Navines, R., Blanco-Hinojo, L., Perez-Garcia, D., Crippa, J., Farre, M., Perez-Jurado, L., Pujol, J., Martin-Santos, R., 2015. Facial emotion processing in patients with social anxiety disorder and Williams-Beuren syndrome: an fMRI study. *J. Psychiatry Neurosci.* 41, 140384.
- Binelli, C., Subira, S., Batalla, A., Muniz, A., Sugranyes, G., Crippa, J.A., Farre, M., Perez-Jurado, L., Martin-Santos, R., 2014. Common and distinct neural correlates of facial emotion processing in social anxiety disorder and Williams syndrome: a systematic review and voxel-based meta-analysis of functional resonance imaging studies. *Neuropsychologia* 64C, 205–217.
- Birn, R.M., Diamond, J.B., Smith, M.A., Bandettini, P.A., 2006. Separating respiratory-variation-related fluctuations from neuronal-activity-related fluctuations in fMRI. *Neuroimage* 31, 1536–1548.
- Brewer, J.A., Garrison, K.A., Whitfield-Gabrieli, S., 2013. What about the “self” is processed in the posterior cingulate cortex? *Front. Hum. Neurosci.* 7, 647.
- Bruhl, A.B., Delsignore, A., Komossa, K., Weidt, S., 2014. Neuroimaging in social anxiety disorder—a meta-analytic review resulting in a new neurofunctional model. *Neurosci. Biobehav. Rev.* 47, 260–280.
- Bruhl, A.B., Rufer, M., Delsignore, A., Kaffenberger, T., Jancke, L., Herwig, U., 2011. Neural correlates of altered general emotion processing in social anxiety disorder. *Brain Res.* 1378, 72–83.
- Buckner, R.L., Sepulcre, J., Talukdar, T., Krienen, F.M., Liu, H., Hedden, T., Andrews-Hanna, J.R., Sperling, R.A., Johnson, K.A., 2009. Cortical hubs revealed by intrinsic functional connectivity: mapping, assessment of stability, and relation to Alzheimer’s disease. *J. Neurosci.* 29, 1860–1873.
- Bullmore, E., Sporns, O., 2009. Complex brain networks: graph theoretical analysis of structural and functional systems. *Nat. Rev. Neurosci.* 10, 186–198.
- Cao, Q., Shu, N., An, L., Wang, P., Sun, L., Xia, M.R., Wang, J.H., Gong, G.L., Zang, Y.F., Wang, Y.F., He, Y., 2013. Probabilistic diffusion tractography and graph theory analysis reveal abnormal white matter structural connectivity networks in drug-naïve boys with attention deficit/hyperactivity disorder. *J. Neurosci.* 33, 10676–10687.
- Cohen, J., 1988. *Statistical Power Analysis for the Behavioral Sciences*. Lawrence Erlbaum Associates, Hillsdale, NJ, pp. 20–26.
- Cremers, H.R., Veer, I.M., Spinhoven, P., Rombouts, S.A., Yarkoni, T., Wager, T.D., Roelofs, K., 2015. Altered cortical-amygdala coupling in social anxiety disorder during the anticipation of giving a public speech. *Psychol. Med.* 45, 1521–1529.
- Danon, L., Diaz-Guilera, A., Arenas, A., 2006. The effect of size heterogeneity on community identification in complex networks. *J. Stat. Mech. Theor. Exp.* 2006, P11010.
- Ding, J., Chen, H., Qiu, C., Liao, W., Warwick, J.M., Duan, X., Zhang, W., Gong, Q., 2011. Disrupted functional connectivity in social anxiety disorder: a resting-state fMRI study. *Magn. Reson. Imaging* 29, 701–711.
- Engel, K., Bandelow, B., Gruber, O., Wedekind, D., 2009. Neuroimaging in anxiety disorders. *J. Neural Transm. (Vienna)* 116, 703–716.
- Etkin, A., Egner, T., Kalisch, R., 2011. Emotional processing in anterior cingulate and medial prefrontal cortex. *Trends Cognit. Sci.* 15, 85–93.
- Etkin, A., Wager, T.D., 2007. Functional neuroimaging of anxiety: a meta-analysis of emotional processing in PTSD, social anxiety disorder, and specific phobia. *Am. J. Psychiatry* 164, 1476–1488.
- First MB, S.R., Gibbon, M., Williams, J.B.W., 1997. *Structured Clinical Interview for DSM-IV Axis I Disorders (SCID)*. American Psychiatric Press, Washington, DC.
- Fornito, A., Yoon, J., Zalesky, A., Bullmore, E.T., Carter, C.S., 2011. General and specific functional connectivity disturbances in first-episode schizophrenia during cognitive control performance. *Biol. Psychiatry* 70, 64–72.
- Fouche, J.P., van Der Wee, N.J., Roelofs, K., Stein, D.J., 2013. Recent advances in the brain imaging of social anxiety disorder. *Hum. Psychopharmacol.* 28, 102–105.
- Fox, M.D., Zhang, D., Snyder, A.Z., Raichle, M.E., 2009. The global signal and observed anticorrelated resting state brain networks. *J. Neurophysiol.* 101, 3270–3283.
- Freitas-Ferrari, M.C., Hallak, J.E., Trzesniak, C., Filho, A.S., Machado-de-Sousa, J.P., Chagas, M.H., Nardi, A.E., Crippa, J.A., 2010. Neuroimaging in social anxiety disorder: a systematic review of the literature. *Prog. Neuropsychopharmacol. Biol. Psychiatry* 34, 565–580.
- Fresco, D.M., Coles, M.E., Heimberg, R.G., Liebowitz, M.R., Hami, S., Stein, M.B., Goetz, D., 2001. The Liebowitz Social Anxiety Scale: a comparison of the psychometric properties of self-report and clinician-administered formats. *Psychol. Med.* 31, 1025–1035.
- Frick, A., Engman, J., Alaie, I., Bjorkstrand, J., Faria, V., Gingnell, M., Wallenquist, U., Agren, T., Wahlstedt, K., Larsson, E.M., Morell, A., Fredrikson, M., Furmark, T., 2014. Enlargement of visual processing regions in social anxiety disorder is related to symptom severity. *Neurosci. Lett.* 583, 114–119.
- Frick, A., Howner, K., Fischer, H., Kristiansson, M., Furmark, T., 2013. Altered fusiform connectivity during processing of fearful faces in social anxiety disorder. *Transl. Psychiatry* 3, e312.
- Gentili, C., Gobbini, M.I., Ricciardi, E., Vanello, N., Pietrini, P., Haxby, J.V., Guazzelli, M., 2008. Differential modulation of neural activity throughout the distributed neural system for face perception in patients with Social Phobia and healthy subjects. *Brain Res. Bull.* 77, 286–292.
- Gimenez, M., Ortiz, H., Soriano-Mas, C., Lopez-Sola, M., Farre, M., Deus, J., Martin-Santos, R., Fernandes, S., Fina, P., Bani, M., Zancan, S., Pujol, J., Merlo-Pich, E., 2014. Functional effects of chronic paroxetine versus placebo on the fear, stress and anxiety brain circuit in Social Anxiety Disorder: initial validation of an imaging protocol for drug discovery. *Eur. Neuropsychopharmacol.* 24, 105–116.
- Gimenez, M., Pujol, J., Ortiz, H., Soriano-Mas, C., Lopez-Sola, M., Farre, M., Deus, J., Merlo-Pich, E., Martin-Santos, R., 2012. Altered brain functional connectivity in relation to perception of scrutiny in social anxiety disorder. *Psychiatry Res.* 202, 214–223.
- Gross, C., Hen, R., 2004. The developmental origins of anxiety. *Nat. Rev. Neurosci.* 5, 545–552.
- Guyer, A.E., Lau, J.Y., McClure-Tone, E.B., Parrish, J., Shiffrin, N.D., Reynolds, R.C., Chen, G., Blair, R.J., Leibenluft, E., Fox, N.A., Ernst, M., Pine, D.S., Nelson, E.E., 2008. Amygdala and ventrolateral prefrontal cortex function during anticipated peer evaluation in pediatric social anxiety. *Arch. Gen. Psychiatry* 65, 1303–1312.
- Hahn, A., Stein, P., Windischberger, C., Weissenbacher, A., Spindelegger, C., Moser, E., Kasper, S., Lanzenberger, R., 2011. Reduced resting-state functional connectivity between amygdala and orbitofrontal cortex in social anxiety disorder. *Neuroimage* 56, 881–889.
- Hamilton, J.P., Chen, M.C., Waugh, C.E., Joormann, J., Gotlib, I.H., 2015. Distinctive and common neural underpinnings of major depression, social anxiety, and their comorbidity. *Soc. Cogn. Affect Neurosci.* 10, 552–560.
- Hattingh, C.J., Ipser, J., Tromp, S.A., Syal, S., Lochner, C., Brooks, S.J., Stein, D.J., 2013. Functional magnetic resonance imaging during emotion recognition in social anxiety disorder: an activation likelihood meta-analysis. *Front. Hum. Neurosci.* 6, 347.
- He, Y., Evans, A., 2010. Graph theoretical modeling of brain connectivity. *Curr. Opin. Neurol.* 23, 341–350.
- Klumpff, H., Angstadt, M., Nathan, P.J., Phan, K.L., 2010. Amygdala reactivity to faces at varying intensities of threat in generalized social phobia: an event-related functional MRI study. *Psychiatry Res. Neuroimaging* 183, 167–169.
- Klumpff, H., Angstadt, M., Phana, K.L., 2012. Insula reactivity and connectivity to anterior cingulate cortex when processing threat in generalized social anxiety disorder. *Biol. Psychol.* 89, 273–276.
- Laeger, I., Dobel, C., Radenz, B., Kugel, H., Keuper, K., Eden, A., Arolt, V., Zwitserlood, P., Dannlowski, U., Zwanzger, P., 2014. Of ‘disgrace’ and ‘pain’ - corticolimbic interaction patterns for disorder-relevant and emotional words in social phobia. *PLoS One* 9, e109949.
- Latora, V., Marchiori, M., 2001. Efficient behavior of small-world networks. *Phys. Rev. Lett.* 87, 198701.
- Liang, X., Zou, Q., He, Y., Yang, Y., 2013. Coupling of functional connectivity and regional cerebral blood flow reveals a physiological basis for network hubs of the human brain. *Proc. Natl. Acad. Sci. U. S. A.* 110, 1929–1934.
- Liao, W., Chen, H., Feng, Y., Mantini, D., Gentili, C., Pan, Z., Ding, J., Duan, X., Qiu, C., Lui, S., Gong, Q., Zhang, W., 2010. Selective aberrant functional connectivity of resting state networks in social anxiety disorder. *Neuroimage* 52, 1549–1558.
- Liao, X., Cao, M., Xia, M., He, Y., 2017. Individual differences and time-varying features of modular brain architecture. *Neuroimage* 152, 94–107.
- Liao, X.H., Xia, M.R., Xu, T., Dai, Z.J., Cao, X.Y., Niu, H.J., Zuo, X.N., Zang, Y.F., He, Y., 2013. Functional brain hubs and their test-retest reliability: a multiband resting-state functional MRI study. *Neuroimage* 83, 969–982.
- Liebowitz, M.R., Gorman, J.M., Fyer, A.J., Klein, D.F., 1985. Social phobia. Review of a neglected anxiety disorder. *Arch. Gen. Psychiatry* 42, 729–736.
- Liu, F., Zhu, C., Wang, Y., Guo, W., Li, M., Wang, W., Long, Z., Meng, Y., Cui, Q., Zeng, L., Gong, Q., Zhang, W., Chen, H., 2015. Disrupted cortical hubs in functional brain networks in social anxiety disorder. *Clin. Neurophysiol.* 126, 1711–1716.
- Lui, S., Zhou, X.J., Sweeney, J.A., Gong, Q., 2016. Psychoradiology: the frontier of neuroimaging in psychiatry. *Radiology* 281, 357–372.
- Lynall, M.E., Bassett, D.S., Kerwin, R., McKenna, P.J., Kitzbichler, M., Muller, U., Bullmore, E., 2010. Functional connectivity and brain networks in schizophrenia. *J. Neurosci.* 30, 9477–9487.
- Majak, K., Pitkanen, A., 2003. Activation of the amygdalo-entorhinal pathway in fear-conditioning in rat. *Eur. J. Neurosci.* 18, 1652–1659.
- Marchand, W.R., 2010. Cortico-basal ganglia circuitry: a review of key research and implications for functional connectivity studies of mood and anxiety disorders. *Brain Struct. Funct.* 215, 73–96.
- Mathew, S.J., Coplan, J.D., Gorman, J.M., 2001. Neurobiological mechanisms of social anxiety disorder. *Am. J. Psychiatry* 158, 1558–1567.
- McClure, E.B., Monk, C.S., Nelson, E.E., Parrish, J.M., Adler, A., Blair, R.J., Fromm, S., Charney, D.S., Leibenluft, E., Ernst, M., Pine, D.S., 2007. Abnormal attention modulation of fear circuit function in pediatric generalized anxiety disorder. *Arch. Gen. Psychiatry* 64, 97–106.
- Murphy, K., Birn, R.M., Handwerker, D.A., Jones, T.B., Bandettini, P.A., 2009. The impact of global signal regression on resting state correlations: are anti-correlated networks introduced? *Neuroimage* 44, 893–905.
- Murphy, K., Fox, M.D., 2016. Towards a consensus regarding global signal regression for resting state functional connectivity MRI. *Neuroimage*. <https://doi.org/10.1016/j.neuroimage.2016.10.111.1052>.
- Onnela, J.P., Saramaki, J., Kertesz, J., Kaski, K., 2005. Intensity and coherence of motifs in weighted complex networks. *Phys. Rev. E Stat. Nonlin. Soft Matter Phys.* 71, 065103.
- Pavuluri, M.N., Herbener, E.S., Sweeney, J.A., 2005. Affect regulation: a systems neuroscience perspective. *Neuropsychiatric Dis. Treat.* 1, 9–15.
- Power, J.D., Barnes, K.A., Snyder, A.Z., Schlaggar, B.L., Petersen, S.E., 2012. Spurious but systematic correlations in functional connectivity MRI networks arise from subject motion. *Neuroimage* 59, 2142–2154.
- Prater, K.E., Hosanagar, A., Klumpff, H., Angstadt, M., Phan, K.L., 2013. Aberrant amygdala-frontal cortex connectivity during perception of fearful faces and at rest in generalized social anxiety disorder. *Depress Anxiety* 30, 234–241.
- Pujol, J., Gimenez, M., Ortiz, H., Soriano-Mas, C., Lopez-Sola, M., Farre, M., Deus, J., Merlo-Pich, E., Harrison, B.J., Cardoner, N., Navines, R., Martin-Santos, R., 2013.

- Neural response to the observable self in social anxiety disorder. *Psychol. Med.* 43, 721–731.
- Robinson, O.J., Charney, D.R., Overstreet, C., Vytal, K., Grillon, C., 2012. The adaptive threat bias in anxiety: amygdala-dorsomedial prefrontal cortex coupling and aversive amplification. *Neuroimage* 60, 523–529.
- Robinson, O.J., Krinsky, M., Lieberman, L., Allen, P., Vytal, K., Grillon, C., 2014. Towards a mechanistic understanding of pathological anxiety: the dorsal medial prefrontal-amygdala 'aversive amplification' circuit in unmedicated generalized and social anxiety disorders. *Lancet Psychiatry* 1, 294–302.
- Rubinov, M., Sporns, O., 2010. Complex network measures of brain connectivity: uses and interpretations. *Neuroimage* 52, 1059–1069.
- Ruscio, A.M., Brown, T.A., Chiu, W.T., Sareen, J., Stein, M.B., Kessler, R.C., 2008. Social fears and social phobia in the USA: results from the National Comorbidity Survey Replication. *Psychol. Med.* 38, 15–28.
- Sladky, R., Hoflich, A., Kublbock, M., Kraus, C., Baldinger, P., Moser, E., Lanzenberger, R., Windischberger, C., 2015. Disrupted effective connectivity between the amygdala and orbitofrontal cortex in social anxiety disorder during emotion discrimination revealed by dynamic causal modeling for fMRI. *Cereb. Cortex* 25, 895–903.
- Stein, M.B., Goldin, P.R., Sareen, J., Zorrilla, L.T., Brown, G.G., 2002. Increased amygdala activation to angry and contemptuous faces in generalized social phobia. *Arch. Gen. Psychiatry* 59, 1027–1034.
- Stein, M.B., Stein, D.J., 2008. Social anxiety disorder. *Lancet* 371, 1115–1125.
- Strogatz, S.H., 2001. Exploring complex networks. *Nature* 410, 268–276.
- Sylvester, C.M., Corbetta, M., Raichle, M.E., Rodebaugh, T.L., Schlaggar, B.L., Sheline, Y.I., Zorumski, C.F., Lenze, E.J., 2012. Functional network dysfunction in anxiety and anxiety disorders. *Trends Neurosci.* 35, 527–535.
- Wang, J., Wang, X., Xia, M., Liao, X., Evans, A., He, Y., 2015. GRETA: a graph theoretical network analysis toolbox for imaging connectomics. *Front. Hum. Neurosci.* 9, 386.
- Wang, J., Zuo, X., Dai, Z., Xia, M., Zhao, Z., Zhao, X., Jia, J., Han, Y., He, Y., 2013. Disrupted functional brain connectome in individuals at risk for Alzheimer's disease. *Biol. Psychiatry* 73, 472–481.
- Watts, D.J., Strogatz, S.H., 1998. Collective dynamics of 'small-world' networks. *Nature* 393, 440–442.
- Weissenbacher, A., Kasess, C., Gerstl, F., Lanzenberger, R., Moser, E., Windischberger, C., 2009. Correlations and anticorrelations in resting-state functional connectivity MRI: a quantitative comparison of preprocessing strategies. *Neuroimage* 47, 1408–1416.
- Xia, M., Wang, J., He, Y., 2013. BrainNet Viewer: a network visualization tool for human brain connectomics. *PLoS One* 8, e68910.
- Yan, C., Zang, Y., 2010. DPARSF: a MATLAB toolbox for "pipeline" data analysis of resting-state fMRI. *Front. Syst. Neurosci.* 4, 13.
- Zalesky, A., Fornito, A., Bullmore, E.T., 2010. Network-based statistic: identifying differences in brain networks. *Neuroimage* 53, 1197–1207.
- Zalesky, A., Fornito, A., Seal, M.L., Cocchi, L., Westin, C.F., Bullmore, E.T., Egan, G.F., Pantelis, C., 2011. Disrupted axonal fiber connectivity in schizophrenia. *Biol. Psychiatry* 69, 80–89.
- Zhang, J., Wang, J., Wu, Q., Kuang, W., Huang, X., He, Y., Gong, Q., 2011. Disrupted brain connectivity networks in drug-naive, first-episode major depressive disorder. *Biol. Psychiatry* 70, 334–342.
- Zhang, Y.X., Zhu, C.Y., Chen, H., Duan, X.J., Lu, F.M., Li, M.L., Liu, F., Ma, X.J., Wang, Y.F., Zeng, L., Zhang, W., Chen, H.F., 2015. Frequency-dependent alterations in the amplitude of low-frequency fluctuations in social anxiety disorder. *J. Affect. Disord.* 174, 329–335.